

M'hamed Mahdad^{1*}, Adel Benidir¹, Idir Belaidi²

¹National Centre of Studies and Integrated Research on Building Engineering CNERIB, Algiers, Algeria

²Department of Mechanical Engineering, University M'hamed Bougara Boumerdes, Algeria

*Corresponding author. E-mail: mahdadcnerib@gmail.com

Received (Otrzymano) 25.08.2021

EXPERIMENTAL AND NUMERICAL EVALUATION OF QUASI-STATIC INDENTATION BEHAVIOUR OF LAMINATES WITH POLYPROPYLENE MATRIX

This paper presents an analysis of the damage process of composite laminates subjected to low-velocity quasi-static indentation (QSI) load. The laminates were prepared using the compression moulding technique. The composites were made from orthotropic layers with E-glass or steel fibres and a polypropylene matrix. The quasi-static indentation tests were carried out at three levels of indentation energy under low-velocity. The experimental results reveal that using steel fibres increases the perforation threshold, which alludes to the importance of the fibre type in delineating damage regions. In contrast, the evolution of the damage and the perforation resistance of glass fibre reinforced laminates is somewhat different. A numerical model based on a finite element program was developed to understand the mechanisms of damage evolution in the laminates. It involves implementing the Matzenmiller-Lubliner-Taylor (MLT) damage model. A comparison between the experimental and numerical results was also made.

Keywords: damage mechanisms, composite materials, quasi-static indentation, finite element

INTRODUCTION

The response of composite materials to mechanical impact is a complex area of investigation as the damage modes could involve various processes [1, 2]. The response of composite materials to impact loading can lead to damage pertaining to three modes of failure: matrix cracking, delamination and eventually fibre breakage for high-energy impacts.

Many studies have confirmed the similarities between quasi-static indentation tests (QSI) and the low-velocity impacts (LVI) for composite laminates [3-5]. It is assumed that for very low-velocity impacts and high impactor-to-target mass ratios, the effect of the structure's inertia is negligible and the problem is essentially quasi-static [6, 7]. As a matter of fact, even though no visible damage is observed around the impact area, matrix cracking and delamination can occur as internal damage is difficult to detect [8, 9]. This internal damage can alter the structural response of composites and could subsequently reduce their structural performance. Furthermore, the initial failure mechanism in the 3-D low-velocity impact event is identified independently from the stacking sequence of the laminates [10]. As a result, this problem of impact on composites has received much more research attention in recent years [11, 12].

The influence of low-velocity impact on the behaviour of composites made from a polypropylene matrix (PP) and E-glass fibre was investigated by Simeoli et al.

[13]. The main conclusions concern management of the resistance of the interface, which can be a viable option for designing composites based on thermoplastics. Therefore, composites could increase their tolerance to the damage of impacts and balanced quasi-static properties. Similarly, Yudhanto et al. [14] showed that woven composites with a PP matrix reinforced with glass fibres have important residual strength and less damage after indentation. The woven composites could resist a large range of indentation loads (12÷30 J). Davies and Olsson [15] examined the behaviour of composite laminate plates subjected to low-velocity impact. The response of the material could produce intermittently three kinds of results, called rebound, stop and perforation, respectively. The classification of those responses is based on the potential energy initially conferred to the impactor by fixing its drop height. It was deduced that if the amount of energy absorbed by the specimen is not excessively high, the impactor would experience rebound. This last contention was also confirmed by Zulkafli et al. [16].

FE-numerical approaches seem to be the best technique for analysing the behaviour of composite laminate plates considering accuracy, cost and time [17, 18]. Many researchers have developed numerous models in aim to predict the behaviour of composites [19, 20]. Tabiei et al. [21] conducted research on predicting delamination in composite laminates with a low-velocity

impact test using a cohesive zone plasticity model (CZM). The conclusion made by Amaro et al. [22] emphasizes the influence of thickness on the impact behaviour during the low-velocity impact of laminated polymer matrix composites. In addition, the damage tolerance of fibre reinforced composites to impact was numerically investigated. The important findings confirm the influence of parameters such as the hygrothermal conditions, the stacking sequence and the impactor geometry [23, 24].

Using the continuum damage mechanics (CDM) approach, Matzenmiller et al. [25] developed a mathematical model for the damage of composite materials called MLT. The main idea behind the construction of that model was to connect the damage level to the degraded elastic properties of the material, which in turn depends on the particular damage mechanism. This approach has been implemented in many research works [26-28], revealing interesting results in predicting the impact response and potential damage. On other hand, Zhu and Yu [29] proposed an analytical model for predicting the low-velocity impact response of fibre-reinforced composite laminated plates, including delamination effects in orthotropic composite plates, which mainly focuses on the relatively weak resistance. It was observed that the variation in the response caused by delamination was apparent on the velocity history curve of the impact point.

The experimental and numerical approach developed as part of this work is based on a study of the nonlinear behaviour of composite materials constituting a polypropylene matrix reinforced with continuous fibres (glass, steel). This approach aims to shed light on the mechanisms of damage and failure through the experimental identification of physical phenomena such as the presence of crack, delamination, and to assess the effect of the damage on the mechanical performance of reinforced laminates.

EXPERIMENTAL PROCEDURE

Materials and preparation

Specimens of polypropylene plates reinforced with glass fibre or stainless-steel fine wire mesh were used in the present study. The polypropylene (PP) granules are those used in the mechanical industry with a density of 0.90 g/cm^3 and melting point of 175°C . The first reinforcement material was E-glass fibre with a density of 2.54 g/cm^3 ; this is the most commonly used glass fibre, which is fire-resistant to a temperature of 830°C . Above this temperature softening and viscous flow begin. Finally, melting occurs at 1070°C . The second reinforcement material was a fine wire mesh of stainless steel with a density of around 7.90 g/cm^3 .

The E-glass/PP (denoted as GFPP) and steel-wire/PP (denoted as SWPP) laminates were manufactured by the compression moulding technique [9, 30]. The E-glass fibre and steel wires were oriented respec-

tively at 0° and 90° in longitudinal and transverse directions, as shown in Figure 1. The stacking sequences used were a quasi-isotropic layup $[0/90^\circ]_{2s}$. The fibre volume fractions (labelled v_f) for the GFPP and SWPP laminates were respectively 48 and 36%.

The preparation process is based on stacking two layers of pre-impregnated woven, symmetrically arranged with respect to the middle plane of the plate. The mould containing the pre-impregnated woven composed of polypropylene (PP) granules and continuous fibres (glass, steel wire) was placed subsequently in an air-circulating oven with an adjusted internal temperature of 180°C . The plates were stamped with a cold press under the pressure of 0.80 N/mm^2 . This fast cooling is recommended to reduce as much possible the crystallinity of the polypropylene matrix. When the mould temperature was less than 55°C , the panels were removed and carefully inspected.

The dimensions of each square plate were $100 \times 100 \text{ mm}$ with a thickness of $4.00 \pm 0.10 \text{ mm}$, obtained after compression moulding.

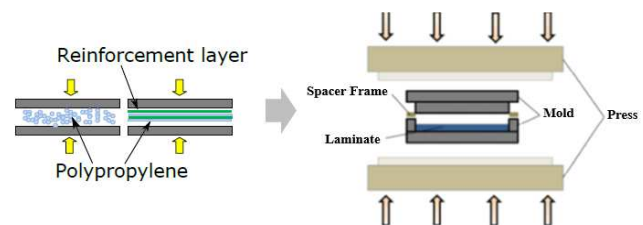


Fig. 1. Stacking sequence of thermoplastic fibre laminate

Quasi-static indentation tests and setup

The quasi-static indentation test consists in subjecting materials to the impact of an indenter. The tests were conducted by mounting an instrumented steel tip with 16-mm diameter in an electromechanical universal testing machine (MTS Criterion series 41) and directing the indenter straight towards the specimen. The details about the setup are shown in Figure 2.

This machine is equipped with *TestSuit* software to program the loads and to define the acquisition frequency. The load cell moves vertically with the indenter at a constant velocity.

A constant crosshead displacement rate of 1.2 mm/min was used in all the tests. The composite plates were clamped between two steel plates in the horizontal direction. The dimensions of the plates were 200 mm in length and width, 10 mm in thickness, which were secured with four bolts (Fig. 2b). Furthermore, in order to perform the indentation test correctly, the steel plates had a circular opening with a diameter of 70 mm . This experimental setup was specially designed and could easily be installed on the MTS machine (Fig. 3).

To determine the conclusive effect of indentation on the composite plates, a series of tests at three energy levels (charge/discharge) were carried out. The indentation energy stages are gradually represented by the penetration depths denoted as H1, H2, and H3 in Figure

2a. H1 and H2 are below the critical maximum energy, H3. The last level of penetration (H3) causes total perforation of the indented sample. Initially, the indenter is positioned at a distance of 4 mm (H0) from the composite laminate.

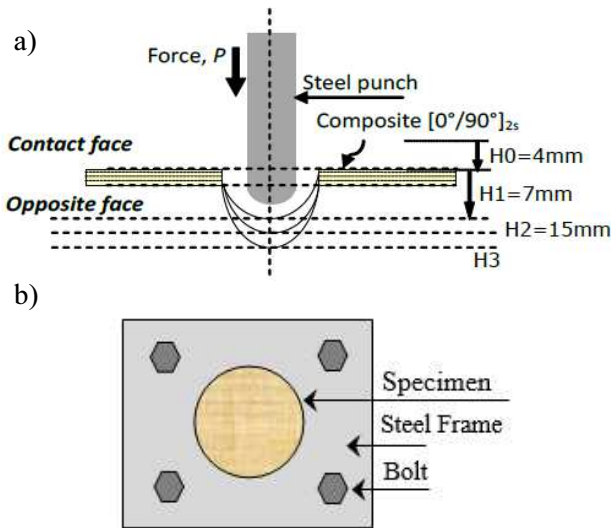


Fig. 2. Specimen clamp and hemispherical-ended projectile (a), laminate mounting (b)

After the first load, the indenter returns to its initial position with H corresponding to $F = 0$ kN. The process is repeated for a second charge in order to reach the second stage. The last stage concerns perforation and penetration of the composite plate. Primarily, the indenter goes down until the distance of $H1 = 7$ mm from the upper surface of the composite laminates. Then it goes back to the initial position. After that, the process is repeated for a second load to attain the second penetration stage limited to $H2 = 15$ mm.

EXPERIMENTAL RESULTS

Figure 4 shows the results of two charge/discharge tests performed on the GFPP and SWPP composite plates at the penetration depth of H1 and H2.

For both tests, the elastic and the anelastic domains are identifiable. The anelastic domain is likely due to the contribution of viscosity (PP matrix), plasticity and damage. The different loadings cause specific residual displacements (noted ϵ_r), depending on the nature of the reinforcement. In fact, as depicted in Figures 4a and 4b, hysteresis appears after each discharge, which results in the occurrence of at least one the classified responses. Hysteresis generally refers to the loss of stiffness as a damage is detected.

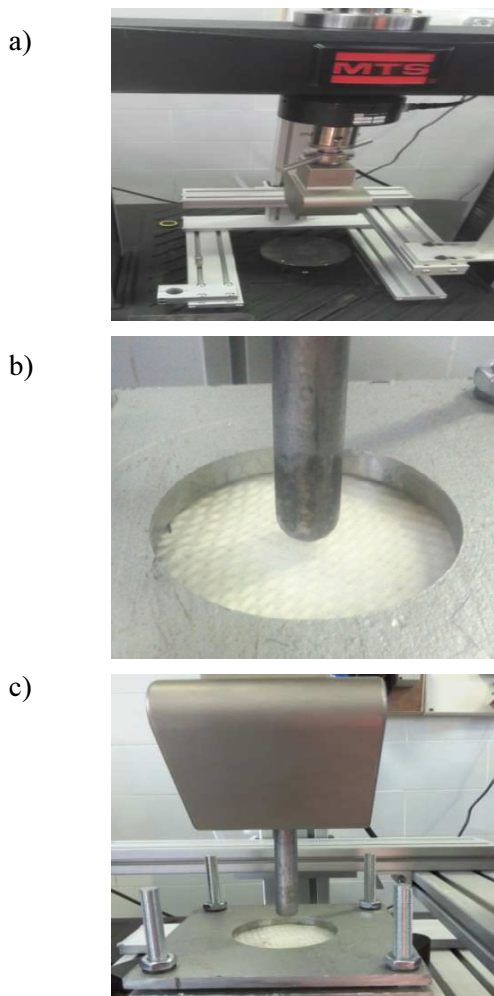


Fig. 3. Mounting brackets and laminate (a), insertion of indenter (b), MTS test machine (c)

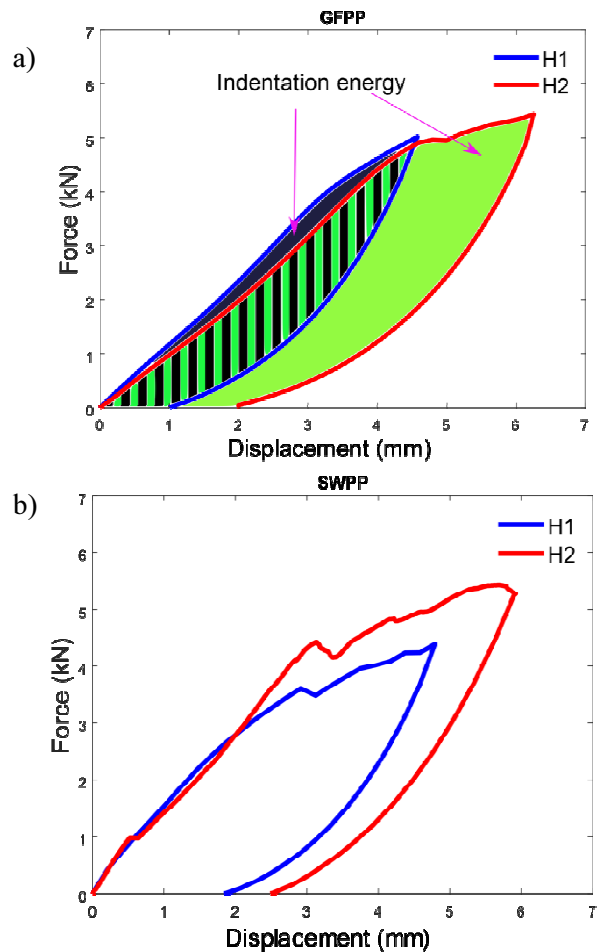


Fig. 4. Force-displacement response of GFPP and SWPP from H1 and H2 levels

The area delimited by the force values represents the indentation energy transferred from the indenter to the composite plate. A part of this energy is absorbed by the composite in the form of damage and plastic deformation. A portion of that part is substantially related to the nature of the reinforcement. The remaining amount of energy is returned to the indenter (recovered or elastic energy). The two composite laminates have different residual displacements. At the first loading (denoted as H1) it is evaluated at $\epsilon_r = 1$ mm for the GFPP plates, and is around $\epsilon_r = 1.8$ mm for the SWPP plates. The order of increase is around 80%. This discrepancy could be explained by the viscoplastic behaviour of the composite, in particular that of the SWPP steel wire (Fig. 4).

However, in the second test, the residual displacement is evaluated on average at $\epsilon_r = 2$ mm for the GFPP plates, while for the SWPP composites it is around $\epsilon_r = 2.8$ mm. The area of the curves increases after each load charge discharge request, which indicates a significant presence of the viscosity effect, in particular in the case of the SWPP plates that show a larger loop (area under the curves).

Regarding the GFPP laminates, the force/displacement evolution occurs in two phases (Fig. 5a). The first phase is elastic, which corresponds to the linear increase in the load, up to the peak at which the maximum load is reached. A non-linear phase follows, characterized by a reduction in load until failure and complete perforation. Nevertheless, it was noted that the laminate was perforated beyond the maximum load, which was reached at 6.2 kN. The observed mechanical behaviour is of a fragile type.

In contrast, the evolution of the load/displacement curve in the SWPP laminate could be described as having three stages (Fig. 5b). The first corresponds to the elastic linear phase where no damage mechanism is detected up to a limit force of about ($F = 4.7$ kN). The latter is equivalent to the charge level corresponding to the initiation of cracks in the upper face. In the second stage (Phase II), the exposed face receives the first damage, characterized by the initiation of matrix cracking. It should also be noted that at this loading level, the reinforcement (steel wire) near the upper face does not show damage.

In the last stage, the increase in the load causes crack propagation in the SWPP laminate. As the incremental load is applied, the steel wires form an obstacle and tend to stop the spread of cracks. That overcomes some fluctuations in the curve with redistribution of the loads over the plate. Failure of the steel wires occurs when the maximum load attains $F = 6.5$ kN. It is worthwhile noting that when the propagation of damage is triggered, the maximum load is accompanied by smooth fluctuations. These fluctuations reported on the force/displacement curve seem originate from the successive failure of the steel wires.

Figure 6a and 6b illustrate the history of the evolution of the indentation load as a function of time for the GFPP and SWPP plates, respectively.

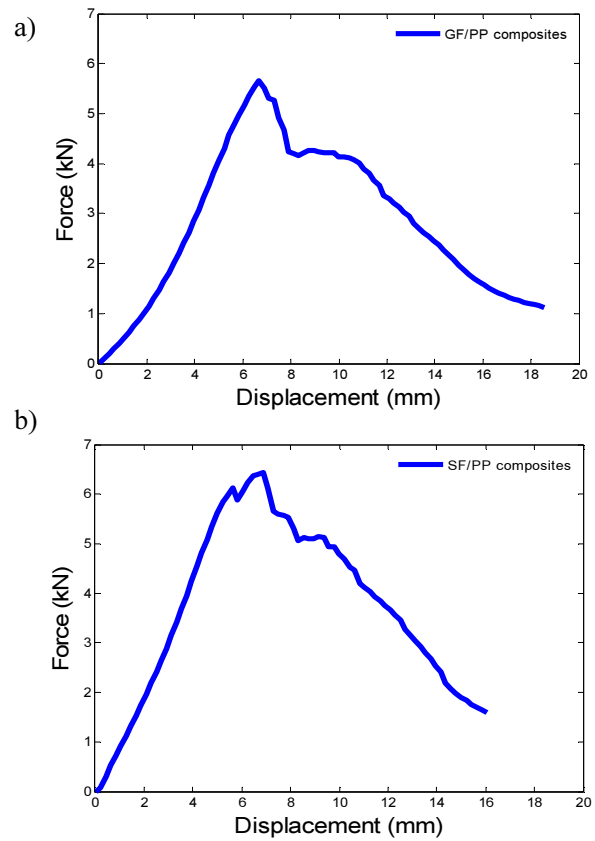


Fig. 5. Load vs. displacement plots of QSI tests at Phase III (H3 level): a) GFPP, b) SWPP

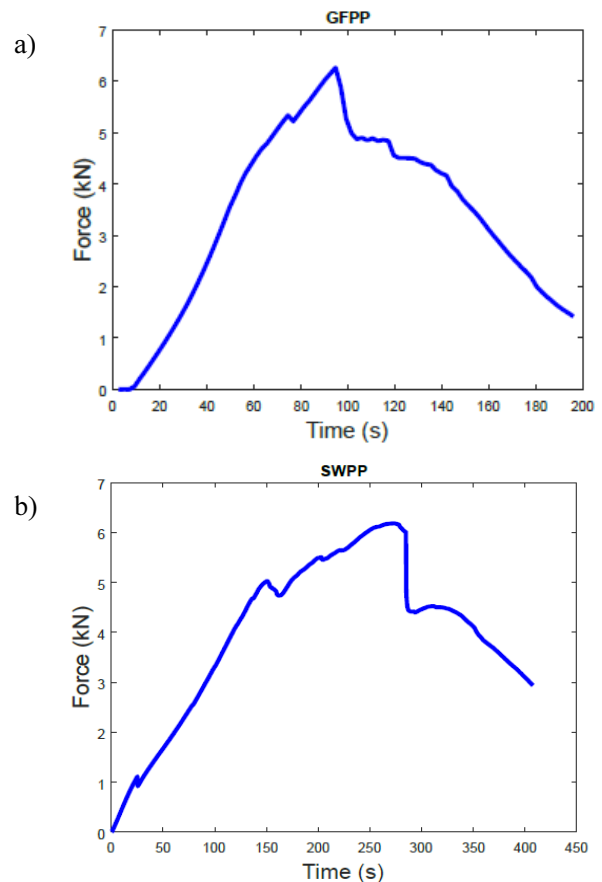


Fig. 6. Indentation (QSI) force-displacement histories of GFPP (a) and SWPP (b) laminates

In the GFPP laminates, the observed mechanical behaviour is of the fragile type. This is due to the nature of the reinforcement that is based on glass fibres, which developed a fragile behaviour. The first damage occurs on the impacted face before the time of 60 seconds. The appearance of damage in the opposite face where the indentation was applied begins thereafter. The drop in resistance at the time of 90 seconds mainly reflects the decrease in the overall stiffness of the plate.

Furthermore, compared to the first case, the evolution of the force/time curve of the SWPP laminate is of the ductile type. This seems to be due to the nature of the reinforcement based on steel wire, which developed ductile behaviour. In addition, as the resistance the composites distinctly falls, the decrease in the overall stiffness of the plate is accompanied by complete perforation of the sample. This conclusion is in concordance with the findings of Carrillo et al. [12] concerning the behaviour of thermoplastic fibre metal composites. The authors highlighted the importance of layup sequences to obtain the highest specific absorbed energy.

Failure mechanisms of indentation tests

To investigate the failure mechanisms at Phase III (H3), the GFPP and SWPP specimens were visually inspected. The analysis of the failure processes in both the front and rear surfaces were considered. As depicted in Figure 7, macroscopic damage in the post-tests could be observed respectively in GFPP and SWPP.

a) GFPP

b) SWPP

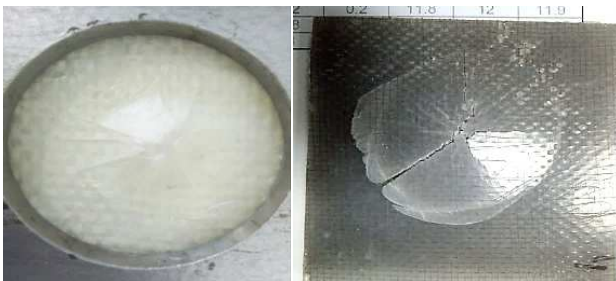


Fig. 7. Representative crack propagation paths on opposite face

In the GFPP composites, the damage is more serious below the average plane under the indentation area, Figure 7a. The damage on the opposite side is characterized by a matrix crack that is initiated with an orientation of $\pm 45^\circ$ in the centre of the indented samples. Shear failure close to the impact location is observed even in the lowermost glass layer with a typical 45° fracture (Fig. 7b).

In the case of the SWPP plates, the damage on the face subjected to impact is characterized by an indentation with nearly circular geometry. The depth of this indentation is proportional to the increase in energy provided by the indenter. Furthermore, the damage to the rear face of the SWPP plates is marked by cracks with a semi-elliptical shape, which are initiated in particular in the centre of the laminates. The appearance of

damage is highlighted by crushing of the PP matrix with considerable delamination and a loss of resistance of the steel wires in both the exposed and opposite sides.

Globally, as observed for SWPP and as supported by other published works [8, 9], the major damage mechanisms identified in laminates when subjected to QSI tests at low-velocity are matrix cracks, delamination, fibre breakage and penetration. Matrix failure and delamination occur during the early stage of impact and are likely to originate from the material property mismatch between the reinforcement and the matrix. In the GFPP, the matrix cracks located on the impact side occur under the impact area due to the high transverse shear stress which is related to the contact shear force and contact area.

NUMERICAL MODEL

Constitutive model and failure criteria

The loading area introduced in the Matzenmiller, Lubliner and Taylor (MLT) model was derived from the Hashin (1980) failure criteria [25, 31]. This failure criteria is used to predict the occurrence of composite plate damage in a complex state of stress [20, 27, 32]. The MLT model includes different parts such as accurate stress analysis, proper failure criteria and material degradation rules. The numerical simulation is performed with the finite element analysis software Abaqus-explicit.

In this study, the MLT model was developed for the non-linear analysis of composite laminates, using damage variables (labelled d_A and d_B). The evolution of these internal variables depends on the stress values defined in the Hashin failure criteria, expressed in stress invariants for a transversely isotropic body and in resistance parameters for the composite [20, 28]. In addition, when one of the Hashin failure criteria is satisfied at a point in a composite structure, it results in damage and can be characterized by the introduction of internal variables for fibre fracture in tension and in compression, cracking of the matrix in tension and compression [26, 27]. Damage affects the warp, weft and shear directions. However, the stress-strain of the laminate is assumed to be elastic orthotropic and the relationship takes the form:

$$\varepsilon = S\sigma \quad (1)$$

where ε and σ are respectively the strain and stress components, S is the compliance matrix for the damaged material.

The compliance matrix is defined by:

$$S = \begin{bmatrix} \frac{1}{(1-d_1)E_1} & -\frac{\nu_{12}}{E_1} & 0 \\ -\frac{\nu_{21}}{E_2} & \frac{1}{(1-d_2)E_2} & 0 \\ 0 & 0 & \frac{1}{(1-d_3)G} \end{bmatrix} \quad (2)$$

where E_1 and E_2 are respectively the elastic moduli in the longitudinal and transverse directions, G is the shear modulus, ν_{12} and ν_{21} are the major and minor Poisson's ratios of undamaged lamina. d_1 is associated with longitudinal (warp) fracture, d_2 is associated with transverse (weft) fracture and d_3 is associated with shear (fibre-matrix) failure [32].

Variable d_A increases continuously with simple exponential damage evolution as specified below [20, 26]:

$$d_{iA} = 1 - \exp \left[-\frac{1}{me} \left(\frac{E_{ii} \varepsilon_{ii}}{\sigma_{f,i}} \right)^m \right] \quad (3)$$

with $m = \frac{1}{\ln \left(\frac{\varepsilon}{\sigma} E \right)}$

where E_{ii} is Young's modulus, $\varepsilon_{ii} (i = 1, 2)$ is the strain related to the progressive damage direction. $\sigma_{i,f} (i = 1, 2)$ is assumed to be identical for compression (longitudinal and transverse, respectively). m is the Weibull modulus, which defined from the strain at maximum stress and Young's modulus E . Thus, the m parameters are defined from the strain value at maximum stress and Young's modulus E . The $d_{i,A}$ damage variable in compression is governed by m parameters that reflect the damage accumulation behaviour.

The damage from the MLT function and the strain softening function must be such that in this approach ($d_A + d_B = 1$) at complete failure (ε_{ult}) [25, 28]. The damage evolution in Zone B is therefore expressed as

$$d_{iB} = \left[\frac{\left(\frac{2G_f}{h_e \sigma_{f,i}} \right)^q}{\left(\frac{2G_f}{h_e \sigma_{f,i}} \right)^q - (\varepsilon_{ii})^q} \left(1 - \frac{(\varepsilon_{ii})^q}{(\varepsilon_{ult})^q} \right) \right]^{\frac{1}{n}} \quad (4)$$

where h_e is the characteristic length of the element, G_f is the fracture energy per unit of area, $\varepsilon_{f,i}$ is the strain at maximum stress, $\frac{2G_f}{h_e \sigma_{f,i}}$ is the strain value ε_{ult} when the specimen is totally damaged.

The explicit finite element (Abaqus/Explicit) was employed for quasi-static indentation test simulation. The GFPP and SWPP laminates are modelled as circular plates, as shown in Figure 8. A refined mesh was created in the vicinity of the indenter, convergence calculation was conducted to ensure that the mesh refinement in the glass/pp and the steel/pp laminates was sufficiently fine enough to capture the stresses and damage with good precision.

The spherical steel indenter with a diameter of 16 mm was also modelled using 8-node linear reduced integration solid elements (C3D8R). The indenter was placed at 0.1 mm above the upper surface of the laminate. During the simulation, the plate was loaded by the

indenter and bounced back when the imposed penetration depth was reached. The simulation was stopped after the indenter returned to its original position.

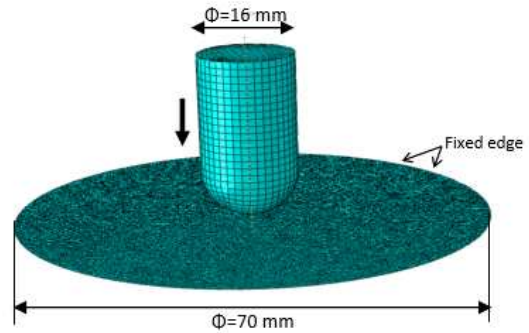


Fig. 8. Numerical FE model of composite plate and hemispherical indenter

The elastic modulus, Poisson's ratio, in addition to the tensile strength and compressive strength of the laminates were obtained from different tests by using contact extensometers [28].

To examine the changes in the failure mechanisms of each material, two contact forces were selected. One was slightly less than the maximum value ($Y_1 = 15$ mm, $Y_2 = 20$ mm) and the other one greater than the maximum value as shown in Figures 9 and 10.

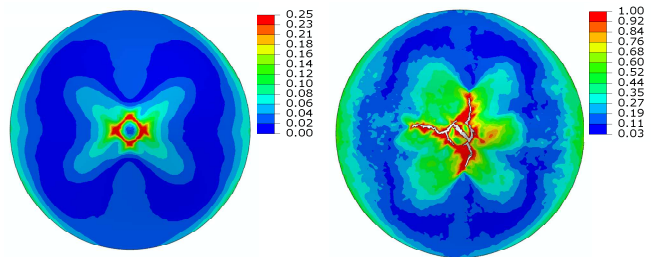


Fig. 9. Damage obtained by numerical simulations for indentation test on GFPP laminate

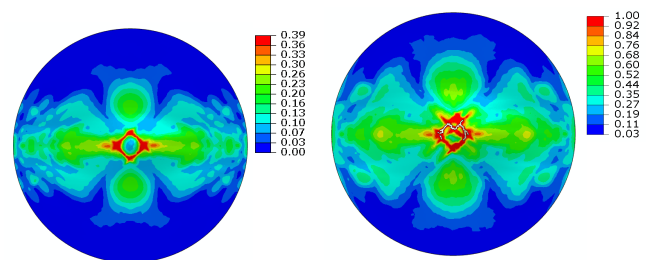


Fig. 10. Evolution of damage area in SWPP laminate

The damage pattern in the two composites is different owing to the high concentration constraints. Due to the higher indentation force, the extent and magnitude of damage at the impact location are higher, especially near the constrained top edge than that shown in Figure 9. In addition, the GFPP exhibited more damage, especially at the indentation location area. Cracking in most cases is along the fibre direction. The closer to the back of the composite, the more serious the damage. The delaminated area is in the shape of double leaf with the

spindle along the fibre direction in the bottom layer, which is consistent with the experimental observation. Similar simulation results have been observed by other authors [27], where the fibre fracture occurs only when large impact energy is applied. Fibre fracture occurs later than that of matrix cracking.

Figure 10 also shows the evolution of indentation as predicted by the numerical model. The predicted post-damage indentation is similar in depth to the actual damage obtained from the experimental results. The appearance of cracks occurs owing to the nonlinear shear damage behaviour of the matrix/fibre interface. In fact, the development of the shear strain overcomes cracking in different directions. This mode of damage releases large amounts of energy, which redistribute the stress over the surfaces of the composites, especially for the SWPP laminate. Thus, this kind of damage results in catastrophic failure of the structure. Compression load in the perpendicular fibre direction causes delamination and leads to the formation of cracks as observed in the experimental results. In addition, with the same initial impactor velocity, the extent of the local peak and the following descent in SWPP decreased with increasing the distance between the impact area and the measurement point. As reported in other works [20, 29], fibre breakage occurs in the later stage of the impact event. The late occurrence of breakage is due to high local stresses as a consequence of the contact between the indenter and the specimen. When fibre failure reaches a critical level, penetration of the indenter leads to macroscopic failure of the composite.

CONCLUSIONS

The present study outlines the experimental characterization of the mechanical response of fibre-reinforced composites under quasi-static indentation load. Numerical investigation was also conducted to predict the orientation of failure. The performances of the GFPP and SWPP composite plates subjected to a quasi-static indentation (QSI) load at low-velocity were characterized in terms of resistance and damage scenarios as well as crack orientation. The level of damage increases with the maximum energy transmitted to the plate. The SWPP laminates exhibited greater damage than the GFPP laminates for all the levels of indentation. Thus, the composite laminate based on the steel fibres exhibited high energy-absorbing levels as a result of shear and delamination failure compared to the glass fibre composite. In the case of the GFPP plates, this damage consists in cracking of the matrix, followed by failure of the fibres distributed over the thickness of the sample.

Good agreement was found between the numerical predictions (MLT model) and the experimental observations. In SWPP, the damage formation is usually from the bottom to the top in a conical form with the back face experiencing fibre fracture and splitting

owing to tensile and shear loading. The GFPP laminates exhibit the formation and propagation of cracks with an angle of approximately 45° to the loading direction. This direction of crack propagation continues thereafter in the direction of fibre orientation

Acknowledgments

The authors would like to thank Dr. A. Mokhtari and Pr. N. Tala Ighil (Research Centre in Industrial Technologies, CRTI, Algeria) for their continuous support of this research project.

REFERENCES

- [1] Abdullah M.R., Cantwell W.J., The impact resistance of polypropylene-based fibre-metal laminates, *Composites Science and Technology* 2006, 66, 1682-1693.
- [2] Bieniaś J., Jakubczak P., Zheng J.Q., Low velocity impact resistance of aluminum/carbon-epoxy fiber metal laminates, *Composite Theory and Practice* 2012, 12(3), 193-197.
- [3] Shuchang J.Q., Xiaohu Y., Xiaoqing Z., Delamination prediction in composite laminates under low-velocity impact, *Composite Structures* 2015, 15, 290-298.
- [4] Jakubczak P., Bieniaś J., Surowska B., Analysis of load-displacement curves and energy absorption relations of selected fibre metal laminates subjected to low-velocity impact, *Composite Theory and Practice* 2014, 14(3), 123-127.
- [5] Sutherland L.S., Soares C.G., Effect of laminate thickness and of matrix resin on the impact of low fibre-volume, woven roving E-glass composites, *Composites Science and Technology* 2004, 64, 1691-1700.
- [6] Olsson R., Mass criterion for wave controlled impact response of composite plates, *Composites Part A* 2000, 31, 879-887.
- [7] Selmy A.I., El-baky M.A.A., Hegazy D.A., Mechanical properties of inter-ply hybrid composites reinforced with glass and polyamide fibers, *Journal Thermoplastic Composite Material* 2019, 32, 267-293.
- [8] Russo P., Acierno D., Simeoli D., Iannace S., Sorrentino L., Flexural and impact response of woven glass fibre fabric/polypropylene composites, *Composites Part B: Engineering* 2013, 54, 415-421.
- [9] Carrillo J., Cantwell G., Mechanical properties of a novel fibre-metal laminate based on a polypropylene composite, *Mechanics of Materials* 2009, 41(7), 828-838.
- [10] Onur Bozkurt M., Parnas L., Coker D., Simulation of drop-weight impact test on composite laminates using finite element method, *Procedia Structural Integrity* 2019, 21, 206-214.
- [11] Mitrevski T., Marshall I.H., Thomson R.S., Jones R., Low-velocity impacts on preloaded GFRP specimens with various impactor shapes, *Composite Structures* 2004, 76(3), 209-217.
- [12] Carrillo J.G., Gonzalez-Canche N.G., Johnson F., Cortes P., Low velocity impact response of fibre metal laminates based on aramid fibre reinforced polypropylene, *Composites Structures* 2019, 220, 708-716.
- [13] Simeoli G., Acierno D., Meola D., Sorrentino L., Iannace S., Russo P., The role of interface strength on the low velocity impact behaviour of PP/glass fibre laminates, *Composites: Part B* 2014, 62, 88-96.
- [14] Yudhanto A., Wafai H., Lubineau G., Goutham S., Mulle M., Yaldiz R., Verghese N., Revealing the effects of matrix

- behavior on low-velocity impact response of continuous fiber-reinforced thermoplastic laminates, *Composite Structures* 2018, 18, 334-72.
- [15] Davies G., Olsson R., Impact on composite structures, *The Aeronautical Journal* 2004, 108, 541-563.
- [16] Zulkafli N., Sivakumar D.M., Sit H.S., Fadzullah M., Razali N., Quasi and dynamic impact performance of hybrid cross-ply banana/glass fibre reinforced polypropylene composites, *Materials Research Express* 2019, 12, 125-344.
- [17] Bouvet C., Rivallant S., Barrau J.J., Low velocity impact modeling in composite laminates capturing permanent indentation, *Composites Science and Technology* 2012, 72, 1977-1988.
- [18] Santiago R.C., Cantwell W.J., Jones N., Alves M., The modelling of impact loading on thermoplastic fibre-metal laminates, *Composite Structures* 2018, 189, 228-238.
- [19] Zhoua J., Wen P., Wang S., Numerical investigation on the repeated low-velocity impact behavior of composite laminates, *Composites Part B: Engineering* 2020, 185, 107-771.
- [20] Warren C., Roberto A., Lopez A., Senthil S., Harun V., Bayraktar H., Progressive failure analysis of three-dimensional woven carbon composites in single-bolt, double-shear bearing, *Composites Part B* 2016, 84, 266-276.
- [21] Tabiei A., Zhang W., Composite laminate delamination simulation and experiment: A review of recent development, *Applied Mechanics Reviews* 2018, 70(3), 030801.
- [22] Amaro P., Reis P., De Moura M., Santos J.B., Influence of the specimen thickness on low velocity impact behavior of composites, *Journal of Polymer Engineering* 2012, 53-58.
- [23] Dogan A., Single and repeated low-velocity impact response of E-glass fiber-reinforced epoxy and polypropylene composites for different impactor shapes, *Thermoplastic Composite Materials* 2019, 1-17.
- [24] Shah S.Z.H., Karuppanan S., Megat-Yusoff P.S.M., Sajid Z., Impact resistance and damage tolerance of fiber reinforced composites: A review, *Composite Structures* 2019, 2017, 100-121.
- [25] Matzenmiller A., Lubliner J., Taylor R.A., Constitutive model for anisotropic damage in fibre composites, *Mechanics of Materials* 1995, 20(2), 125-152.
- [26] Mokhtari A., Ould Ouali M., Tala-Ighil N., Damage modelling in thermoplastic composites reinforced with natural fibres under compressive loading, *International Journal of Damage Mechanics* 2015, 24(8), 1-22.
- [27] Guo W., Xue P., Yang J., Nonlinear progressive damage model for composite laminates used for low velocity impact, *Applied Mathematics and Mechanics* 2013, 34, 1145-1154.
- [28] Mahdad M., Ait Saada A., Belaidi I., Mokhtari A., Benidir A., Damage modelling in thermoplastic laminates reinforced with steel and glass fibres under quasi-static indentation loading at low-velocity, *Advanced Composite Letters* 2018, 27(6), 251-260.
- [29] Zhu Q., Yu Z., A perturbation-based model for the prediction of responses involving delamination during small mass impacts on orthotropic composite plates, *Composites Science and Technology* 2021, 208, 108754.
- [30] Reyes G., Gupta S., Manufacturing and mechanical properties of thermoplastic hybrid laminates based on DP500 steel, *Composites Part A: Applied Science and Manufacturing* 2009, 40(2), 176-183.
- [31] Hashin Z., Failure criteria for unidirectional fibre composites, *Journal of Applied Mechanics* 1980, 47, 321-329.
- [32] Tsai S., Wu E., A general theory of strength for anisotropic materials, *Journal of Composite Materials* 1971, 5, 58-80.